

# Organization-Induced Charge Redistribution in Self-Assembled Organic Monolayers on Gold

S. G. Ray,<sup>†</sup> H. Cohen,<sup>‡</sup> and R. Naaman<sup>\*,†</sup>

*Department of Chemical Physics and Chemical Research Support, Weizmann Institute, Rehovot 76100, Israel*

Haiying Liu<sup>§</sup> and D. H. Waldeck

*Department of Chemistry, University of Pittsburgh, Pittsburgh, Pennsylvania 15260*

*Received: January 23, 2005; In Final Form: May 5, 2005*

The charge redistribution that occurs within dipolar molecules as they self-assemble into organized organic monolayer films has been studied. The extent of charge transfer is probed by work function measurements, using low-energy photoelectron spectroscopy (LEPS), contact potential difference (CPD), and X-ray photoelectron spectroscopy (XPS), with the latter providing fine details about the internal charge distribution along the molecule. In addition, two-photon photoelectron spectroscopy is applied to investigate the electronic structure of the adsorbed layers. We show that charge transfer acts to reduce the dipole–dipole interaction between the molecules but may either decrease or increase the molecule-to-surface dipole moment.

## Introduction

The understanding and control of the electronic properties of solid surfaces and interfaces are important on both a fundamental and a practical level.<sup>1–3</sup> Numerous photoelectron emission studies address the effects of adsorbed molecules on the work function (WF) of the metal substrate.<sup>4</sup> In the X-ray photoelectron spectroscopy (XPS) and ultraviolet photoelectron spectroscopy (UPS) literature,<sup>5,6</sup> it is widely appreciated that the WF of a substrate depends on the conditions of the surface, both morphological and chemical.

Adsorption of molecules or atoms on a metal surface can affect the electronic properties of the surface in several ways. It is well-known that if a dipole layer is formed by the adsorbates, a force is exerted on the electrons while passing through the layer and the energy required to remove an electron from the substrate (that is, the WF) depends on the dipole layer. When atoms are adsorbed on the surface, the dipole layer arises from either charge transfer between the substrate and the adsorbate layer or an induced polarization in the atom. This effect in atoms and the limit on the strength of the dipole density are well-known.<sup>7</sup> When molecules are adsorbed, the situation is different, since a dipole layer can be formed even without charge transfer or polarization. This is due to the intrinsic dipole moment of the molecules.

Close-packed, organized organic layers have been the focus of substantial studies in recent years because of their ability to modify electronic properties of substrates,<sup>8,9</sup> metals or semiconductors,<sup>10–12</sup> in a controlled manner and their application as elements in electronic devices,<sup>13–16</sup> light-emitting diodes,<sup>17</sup> sensors,<sup>18</sup> etc. It is usually assumed that the electronic properties of the molecules within a close-packed layer are similar to those of the single adsorbed molecule, namely, that the organization of the layer and its close packing do not affect the electronic

properties of the molecules. The weak coupling between the neutral, ground-state molecules in a monolayer supports this notion and is taken as a justification for using statistical sums of molecular properties to predict the monolayer properties.<sup>19,20</sup> Fundamental considerations indicate that, in the pseudo-two-dimensional structure of organized organic thin films (OOTF), the large electrostatic interaction between molecules can give rise to collective electronic properties that are not a simple average of the individual molecule properties.<sup>21,22</sup>

The dipole–dipole interaction and its electrostatic energy are known to affect the structure of organized close-packed films. For example, McConnell and Boker<sup>23</sup> and Möhwald<sup>24</sup> explained the structure of phospholipids on water as a balance between the molecular dipole–dipole interaction forces and the line tension. For such systems, minimizing the free energy of the layer generates different domain shapes and sizes. In these analyses, the dipole moment of the molecules in the layer was assumed to be constant and the interaction with the substrate (water in most cases) included the image charges. Although these approximations may be accurate for lipid bilayers, more recent theoretical work shows that a close-packed layer of dipolar molecules with a large enough dipole moment perpendicular to a metal surface minimizes its free energy by charge transfer from the substrate.<sup>22</sup> Some recent experiments seem to provide direct evidence for this effect, although the results were not interpreted in this way.<sup>25</sup>

Here, we present experimental evidence for charge transfer between organic thiols and a Au substrate upon formation of OOTF. The information on the charge transfer is derived from low-energy photoelectron spectroscopy (LEPS),<sup>26</sup> contact potential difference (CPD),<sup>27</sup> and a new technique based on X-ray photoelectron spectroscopy (XPS), measuring changes in the WF<sup>28</sup> of a gold substrate upon formation of self-assembled monolayer films of polar organic molecules. The two-photon photoelectron (TPPE) spectroscopy method was applied to investigate the electronic structure of the adsorbed layer. The experimentally determined features of the charge distribution in some of the Au/OOTF can be rationalized by simple packing

\* Corresponding author. E-mail: ron.naaman@weizmann.ac.il.

<sup>†</sup> Department of Chemical Physics.

<sup>‡</sup> Chemical Research Support.

<sup>§</sup> Current address: Department of Chemistry, Michigan Technological University, Houghton, MI 49931.

**TABLE 1: Molecules Studied, Their Structure and Calculated Dipole Moment, and the Measured Dipole Moment of the Adsorbed Molecules**

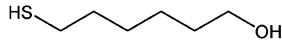
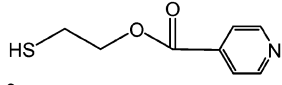
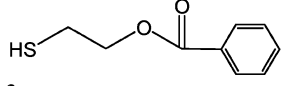
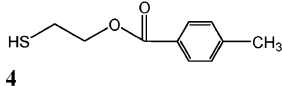
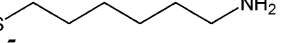
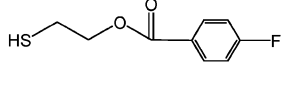
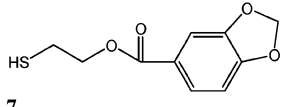
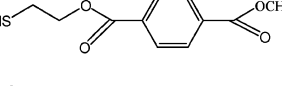
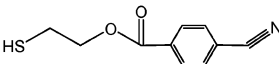
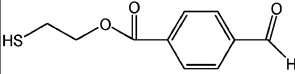
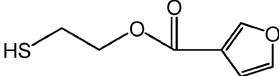
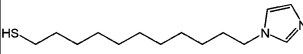
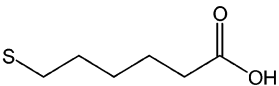
Molecule	Change in Workfunction (eV) <sup>a</sup> ± 30 meV	Calculated total Dipole (Debye) <sup>b</sup> ± 0.4 D		Calculated Component of the dipole perpendicular to the surface. ( $\mu_{\text{per}}$ ) (Debye) <sup>c</sup> ± 0.4 D	Measured $\mu_{\text{per}}$ (Debye) <sup>d</sup> ± 0.4 D
 <b>1</b>	-0.14	STO-3G	2.42	-1.58	-0.2
		6-31G* CM2	2.47	-0.554	
		MIDI CM2	2.23	-0.79	
 <b>2</b>	0.10	STO-3G	1.1	0.05	0.15
		6-31G* CM2	2.45	1.6	
		MIDI CM2	1.66	0.47	
 <b>3</b>	-0.16	STO-3G	2.64	-1.93	-0.23
		6-31G* CM2	2.63	-1.04	
		MIDI CM2	3.8	-2.46	
 <b>4</b>	-0.25	STO-3G	3.0	-2.28	-0.36
		6-31G* CM2	3.11	-1.73	
		MIDI CM2	4.7	3.46	
 <b>5</b>	-0.14	STO-3G	1.9	-0.75	-0.2
		6-31G* CM2	2.41	-0.71	
		MIDI CM2	2.34	-1.2	
 <b>6</b>	0.28	STO-3G	1.82	-1.15	0.4
		6-31G* CM2	2.63	-1.81	
		MIDI CM2	1.76	-0.14	
 <b>7</b>	-0.24	STO-3G	2.23	-1.8	-0.35
		6-31G* CM2	0.45	-0.023	
		MIDI CM2	0.66	-0.51	
 <b>8</b>	0.69	STO-3G	2.47	0.36	1.0
		6-31G* CM2	5.23	2.63	
		MIDI CM2	4.54	0.99	

TABLE 1 (Continued)

Molecule	Change in Workfunction (eV) <sup>a</sup> ± 30 meV	Calculated total Dipole (Debye) <sup>b</sup> ± 0.4 D	Calculated Component of the dipole perpendicular to the surface. ( $\mu_{\text{per}}$ ) (Debye) <sup>c</sup> ± 0.4 D	Measured $\mu_{\text{per}}$ (Debye) <sup>d</sup> ± 0.4 D
 <b>9</b>	0.67	STO-3G	1.85	1.3
		6-31G* CM2	4.51	3.78
		MIDI CM2	2.42	1.84
 <b>10</b>	-0.03	STO-3G	1.67	-0.9
		6-31G* CM2	2.55	-1.76
		MIDI CM2	1.84	-0.26
 <b>11</b>	-0.04	STO-3G	2.33	-1.63
		6-31G* CM2	1.34	-0.038
		MIDI CM2	1.48	-0.54
 <b>12</b>	-0.34	STO-3G	4.8	1.51
		6-31G* CM2	Not calculated	-
		MIDI CM2	4.09	2.74
 <b>13</b>	-0.02	STO-3G	2.7	-1.54
		6-31G* CM2	2.28	-0.075
		MIDI CM2	2.38	-0.22

<sup>a</sup> The average change in the WF,  $\Delta\phi = \phi_{\text{Au+monolayer}} - \phi_{\text{Au}}$ , as measured by the four different methods. <sup>b</sup> The calculated dipole moment of the isolated molecules. For all thiols, the isolated molecule was assumed to have the -SH group. The CM2 calculations were performed using GAMESSPLUS.<sup>37</sup> <sup>c</sup> The calculated dipole moment of the molecule perpendicular to the surface is  $\mu_{\text{per}} = \mu_{\text{||}} \cos \theta$  when  $\mu_{\text{per}}$  and  $\mu_{\text{||}}$  are the total dipole moment perpendicular to the surface and the dipole moment parallel to the molecular axis, respectively. We assume that  $\theta = 30^\circ$ . <sup>d</sup> The dipole moment obtained based on the change in the WF (eq 1). We assumed a density of  $\rho = 4 \times 10^{14}$  molecules/cm<sup>2</sup> and  $\epsilon$  equal to 2.2.<sup>41</sup> The tilt angle was taken to be  $30^\circ$ . <sup>e</sup> The CM2 calculations were performed using GAMESSPLUS.<sup>37</sup>

of adsorbate molecules with their gas-phase dipole moment. For other systems, the observed features require charge redistribution in the molecule and/or with the surface.

## Experimental Section

Some of the compounds used were synthesized and others were purchased. Compounds **2**, **3**, **4**, **6**, **7**, **8**, **9**, **10**, and **11** (see

Table 1) were synthesized and characterized in a manner described previously.<sup>29</sup> Compound **5** (6-aminohexanethiol) was prepared according to the literature method.<sup>30</sup> Preparations of compound **1** (6-(6-hydroxyhexyldisulfanyl)hexan-1-ol)<sup>31</sup> and of compound **12** (1-(11-mercaptoundecyl)imidazole)<sup>32</sup> have been reported previously. Compound **13** (6-mercaptohexanoic acid) was purchased from Aldrich.

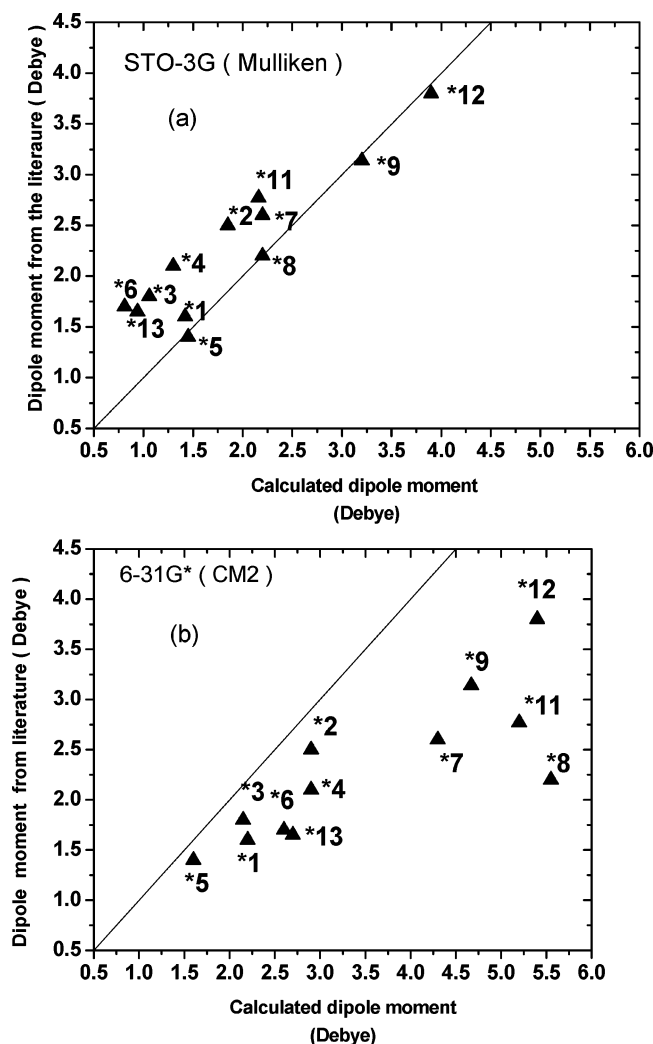


**Figure 1.** Graphs plotting experimental dipole moment values for the molecules in Table 2 (see Table 2 for values and literature references) versus calculated values by (a) the STO-3G/Mulliken method and (b) the 6-31G\*/CM2 method. A line of unit slope is drawn on each graph. Systematic deviation of the calculated value from the experimental value is evident in each case.

The organized organic films were self-assembled on a 200-nm-thick gold film, which was deposited on a 40-nm chromium coated glass slide (Metallhan del Schröer GmbH). The gold samples were cleaned using a published protocol.<sup>33</sup> They were placed for 25 min in an ultraviolet ozone cleaner (Uvocs Inc., model No.-T10X10/OES/E) and then immersed for 20 min in absolute ethanol (Merck). Finally, they were rinsed with ethanol and immersed immediately for 12–16 h in the adsorption solution, which contained 1 mM of the molecules in ethanol. Absolute ethanol (Merck, extra pure) was used as a solvent. After the adsorption, the samples were removed from the solution, rinsed, and blown dry with 99.999% dry nitrogen.

Physical characterization was performed by contact-angle and ellipsometric methods. Static contact-angle measurements were performed with an automated goniometer (Rame-Hart, Model-100). Approximately 3  $\mu$ L of ultrapure water (Millipore Inc.) was deposited onto the sample using a microsyringe. Measurements were recorded immediately after deposition. The layer thickness was measured using an M 2000V (J. A. Wollam Co. Inc.) spectroscopic ellipsometer with a spectral range from 370 to 1000 nm. The data were simulated using Wvase32 software over all wavelengths to fit with the experimental parameters.

Analysis of these data show that the surface coverage varies by less than 25%.

XPS measurements were performed on a Kratos Analytical AXIS-HS instrument using a monochromatized Al ( $K\alpha$ ) source at a relatively low power, 75 W, and a pass energy ranging from 20 to 80 eV. In most samples, these measurements show some extra oxygen signals, assigned to OH groups. Although the S, N, and COO signal intensities are found to agree with the expected atomic ratios, in some cases an extra carbon signal has been detected.<sup>34</sup>

The first method for WF evaluation using XPS was based on measuring the low-energy onset of the photoelectron spectrum. These measurements were performed under a sample bias of  $-20$  V using a small area aperture, a single detector, and a pass energy of 5 eV. An additional novel method for WF studies using a soft e-beam as a potential reference has been applied as well.<sup>28</sup>

Beam-induced degradation during the XPS measurements was followed systematically. Generally, only minor changes in the surface composition were observed on a time scale of 6–8 h. Specifically, the WF evaluation was performed on a short time scale ( $<10$  min), and therefore, the values given below can be considered damage free. On the other hand, small XPS signals (e.g., N(1s)) required relatively long exposure times and such samples were subjected to some degradation. The effect of the degradation was followed by sequential recording of the WF and the XPS signals as a function of exposure time, and the data have been corrected accordingly.<sup>35</sup>

The CPD was measured between a gold substrate coated with the monolayer and a clean gold plate placed parallel to the monolayer surface. A commercial Kelvin probe setup (delta-Phi, Germany) was used. The distance between the sample and the reference gold was sinusoidally varied, thus inducing an oscillating alternating current (ac). The ac is nullified by adjusting the direct current (dc) bias voltage, so that no net charge resides on either surface. This dc bias is then the CPD.<sup>27</sup> The method is contact free, and the measurements were performed in an ultrahigh vacuum (UHV) chamber under a pressure of less than  $10^{-8}$  mbar. The measured change in the WF (reported in Table 1) is given by

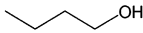
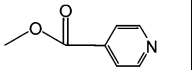
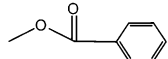
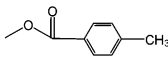
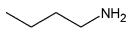
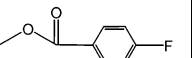
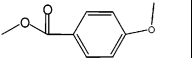
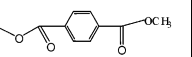
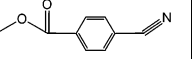
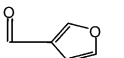
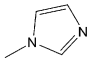
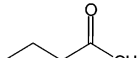
$$\Delta\phi = \phi_{\text{Au+monolayer}} - \phi_{\text{Au}} = \text{CPD}_{\text{Au}} - \text{CPD}_{\text{Au+monolayer}}$$

The low-energy photoelectron transmission studies were performed in a similar UHV chamber. The photoelectrons were ejected from the substrate by irradiation from a laser source (Excimer laser, Lambda Physik) at 193 nm with energies of about 25 pJ/pulse. For the TPPE spectroscopy, the third harmonic of a Nd:Yag laser was used (355 nm), with typical energies of 18  $\mu$ J/pulse. In both cases, the laser pulses are about 15 ns in duration. The photoelectron energy distribution was analyzed using a time-of-flight spectrometer with a typical resolution of 40 meV.<sup>26</sup>

## Calculations

All quantum mechanical calculations were performed using the PC GAMESS version of the GAMESS<sup>36</sup> package and the GAMESSPLUS<sup>37</sup> package using the CM2 method, which is considered one of the best methods for calculating dipole moments.<sup>38</sup> Ab initio calculations were performed using the closed-shell restricted Hartree–Fock (RHF) approximation with three different basis sets: an STO-3G basis set in the GAMESS package<sup>39</sup> and the 6-31G\* and MIDI basis sets using the GAMESSPLUS package. Geometry optimizations utilized

TABLE 2: Experimental and Calculated Dipole Moments of Analogue Molecules

Molecules <sup>a</sup>	Structure	Experimental $\mu$ <sup>b</sup> (D)	Calculated $\mu$ <sup>c</sup> (D)	Calculated $\mu$ <sup>d</sup> (D)
			Mulliken (STO-3G)	CM2(6-31G*)
1*		1.6 to 1.7	1.42	2.2
2*		2.5 <sup>f</sup>	1.85	2.9
3*		1.8 to 1.9	1.06	2.2
4*		2.05 to 2.1	1.3	2.9
5*		1.3 to 1.4	1.45	1.6
6*		1.7 to 1.8	0.81	2.6
7*		2.6	2.2	4.3
8*		2.2	2.2	5.6
9*		3.14 <sup>e</sup>	3.2	4.7
11*		2.77	2.16	5.2
12*		3.6 to 3.8	3.9	5.4
13*		1.65 <sup>g</sup>	0.94	2.7

<sup>a</sup> The \* symbol represents similar molecules; for example, 1\* represents a molecule similar in structure to molecule number 1. <sup>b</sup> Values were obtained from Beilstein Crossfire Database, which is based on *Beilstein's Handbuch der Organischen Chemie*, unless otherwise noted. <sup>c,d</sup> Calculations were performed using the HF, Mulliken (STO-3G), and CM2 (6-31G\*) methods, respectively, in the same manner used for the compounds in Table 1. <sup>e</sup> Friedl, Z.; Exner, O. *Collect. Czech. Chem. Commun.* **1978**, 43, 2591. <sup>f</sup> Rospenk, M.; Szemik, A.; Kyuskens, P. *J. Mol. Struct.* **1985**, 129, 333. <sup>g</sup> Kovrigina, L. P.; Bogdanov, L. I. *Russ. J. Phys. Chem.* **1970**, 44, 881.

standard gradient methods. For calibrating the different calculation methods, we compared the calculated values to those available from experiments for several molecules which are similar to those used in the experiment. Table 2 presents the molecules, the calculated values, and the experimental ones. Figure 1 shows the correlation between the experimental and calculated values for the STO-3G/Mulliken method and for the 6-31G\*/CM2 method. Clearly, while using the first method, the calculated values tend to exceed the experimental ones; the opposite is true when we use the second method. Table 2 shows the calculated dipole moment using the two methods for the molecules used in the adsorption experiments. All calculations were performed for an isolated molecule.

## Results

The WF changes of the monolayer coated gold samples were measured using four different methods: CPD, LEPS, high-energy photoelectron spectroscopy using the XPS system, and

local electrostatic potential changes using the XPS spectra.<sup>28</sup> Figure 2 presents the LEPS spectra for which the low-energy cutoff of a spectrum is associated with the WF of that sample.<sup>26a</sup> The WF obtained for each type of film (i.e., molecular composition) can vary by up to  $\pm 50$  meV, depending on the method and the batch. This variation has two primary sources: (1) the reference bare gold sample used in each method changes, so that the reference point can be different, and (2) the quality of the monolayer varies between batches. Table 1 shows the changes in WF for all molecules, averaged over the values obtained by all four methods, and the calculated values obtained by the two methods.

**Effective Dipole Moments.** The change in the WF is related to the dipole moment density perpendicular to the surface through the relation<sup>40</sup>

$$\Delta\Phi = \frac{\mu N \cos \theta}{\epsilon \epsilon_0} \quad (1)$$



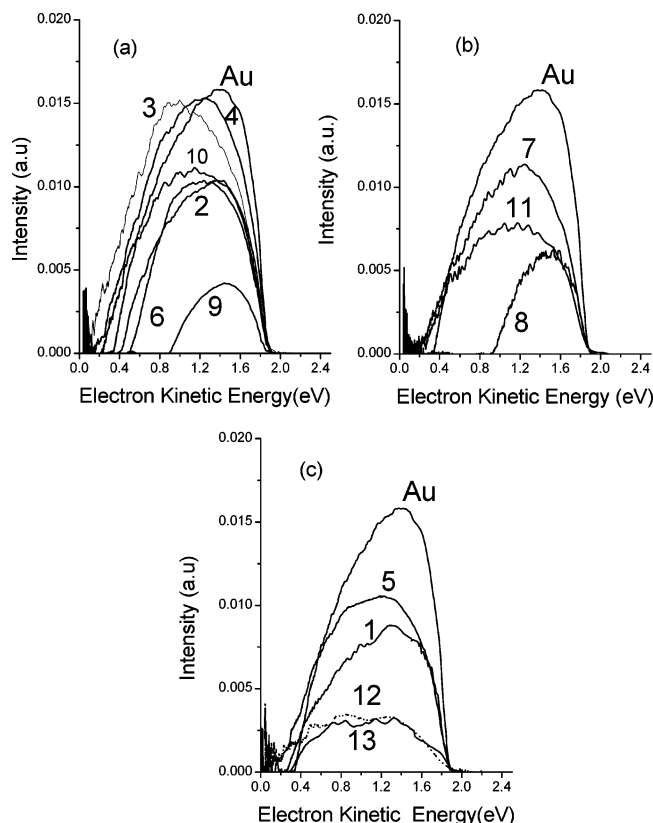


**Figure 2.** LEPS spectra for SAMs composed of each of the compounds in Table 1. The laser excitation energy was 6.42 eV. In each panel, the LEPS for bare Au is shown as a reference. The spectra are labeled by the number of the molecule which comprises the layer.

in which  $N$  is the surface density of dipoles (in  $\text{m}^{-2}$ ),  $\mu$  is the effective dipole moment of the molecule (in  $\text{C m}$ ),  $\epsilon_0$  is the permittivity of the vacuum,  $\epsilon$  is the dielectric constant of the layer, and  $\theta$  is the tilt angle of the molecule with respect to the surface normal. Assuming a molecular density that corresponds to an area of  $25 \text{ \AA}^2$  per thiol group, namely,  $4 \times 10^{14}$  molecules/ $\text{cm}^2$ , and  $\epsilon$  equal to 2.2,<sup>41</sup> the component of the dipole moment perpendicular to the surface,  $\mu_{\text{per}}$ , was calculated from the measured changes in the WF. The use of an effective dielectric constant for the film accounts for the well-known depolarization of a dipole by the surrounding dipoles.<sup>7</sup> These values for the dipole moment (in debye;  $1 \text{ D} = 3.336 \times 10^{-30} \text{ C m}$ ) perpendicular to the surface per molecule are reported in Table 1 and Figure 3.

Figure 4 shows a schematic diagram of the adsorbed molecule and its alignment, defined by the tilt and twist angles. The projection of the off-axis dipole component (perpendicular to the molecular axis) on the vertical direction (the surface normal) depends on the twisting angle,  $\varphi$ . Hence, assuming that  $\varphi$  varies randomly among the different domains, the off-axis component of the dipole averages to zero, and the only contribution to be considered is the projection of the axial dipole component (along the molecule axis) on the surface normal. We assume a tilt angle of  $30^\circ$  ( $\theta = 30^\circ$ ) relative to the surface normal, as established in the literature<sup>25</sup> and by our ellipsometry measurements. The sign of the dipole moment is chosen to be positive when the dipole's positive pole is near the surface, which corresponds to an increase in the WF. Figure 3 compares the calculated dipole moments perpendicular to the substrate ( $\mu_{\text{per}}$  component for the isolated molecules) with the dipole moments obtained from the WF change caused by the adsorbed molecules. When the molecule's long axis is tilted at an angle  $\theta$ , with respect to the

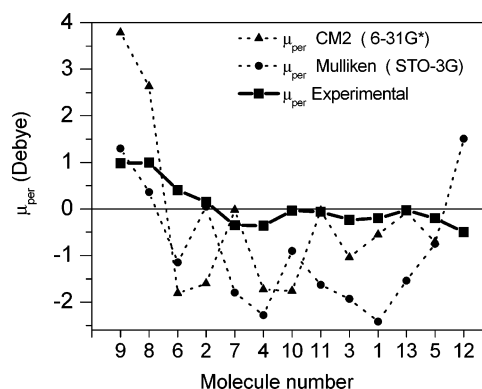


**Figure 3.** Dipole moment (perpendicular to the substrate surface,  $\mu_{\text{per}}$ ) of isolated molecules, calculated using the CM2 method (triangles) and the Mulliken method (circles). The experimentally inferred dipole moment,  $\mu_{\text{per}}$ , of the adsorbed molecules is shown (squares), calculated based on eq 1 and assuming the coverage of  $4 \times 10^{14}$  thiols/ $\text{cm}^2$ . The tilt angle,  $\theta$ , was assumed to be  $30^\circ$ .

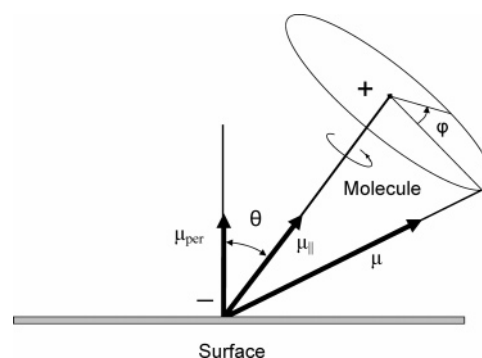


**Figure 4.** Schematic diagram of the dipole moment orientation for adsorbed molecules. The dipole moment is pointing toward the positive pole,  $\theta$  is the tilting angle, and  $\varphi$  is the twist angle.

surface normal, the values for the dipole moment perpendicular to the surface,  $\mu_{\text{per}}$ , are  $\mu_{\text{per}} = \mu_{\text{||}} \cos \theta$ , where  $\mu_{\text{||}}$  is the dipole moment parallel to the molecular axis.

Both Figure 3 and Table 2 demonstrate that, for many of the studied molecules, the experimentally determined dipole moments are smaller than those calculated for the isolated molecules. This is true even for the calculations done using the 6-31G\* (CM2) method, which underestimate the real dipole moment.

Comparing the different functionalized alkanethiols (molecules 1, 13, 5, and 12), it is clear that the experimentally determined perpendicular dipole component for 1, 13, and 12 is significantly smaller than the one calculated using the STO-3G/Mulliken method. For molecule 12, in addition to the difference in dipole magnitude, the sign of the calculated dipole moment is opposite to the sign actually measured.

When comparing the molecules that contain an aromatic group, the picture is more complicated. In most cases, the measured dipole moment is smaller than the one calculated by the STO-3G/Mulliken method (molecules 7, 4, 10, 11, and 3). For molecules 2 and 9, the value of the measured dipole moment is similar to the theoretical value, and for molecule 6, the sign of the experimental dipole moment is opposite to that of the theoretical prediction. The experimental value obtained for molecule 8 falls between the calculated values as obtained by the two different calculation methods. When comparing the experimental values to those calculated by the 6-31G\*/CM2 method, the same discrepancy persists for molecules 4, 10, 3, and 6, while for 7 and 11 the experimental and theoretical values

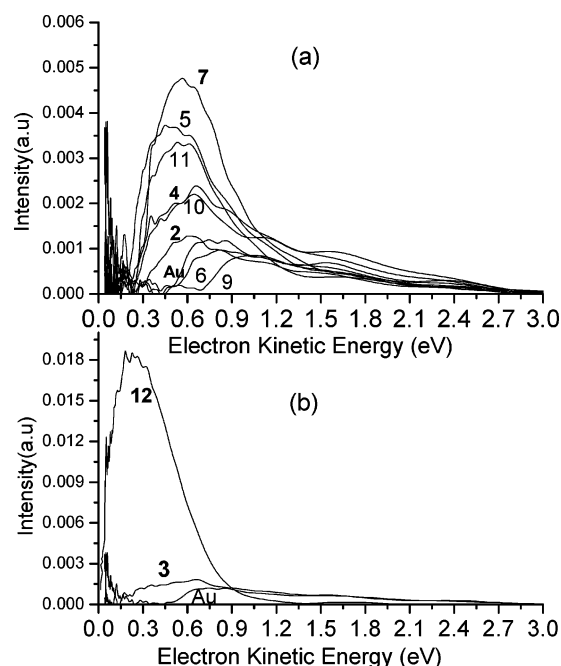


**Figure 5.** TPPE spectra obtained using a photon energy of 3.55 eV. Each curve is labeled by the molecule comprising the monolayer.

are quite close. In the case of molecule **2**, the measured dipole is much smaller than the one calculated.

From Figure 3, a general trend can be recognized, which indicates a reduction of the effective dipole moment of the adsorbed molecules relative to the calculated dipole moment of the isolated molecule. Moreover, not only the magnitude but sometimes even the sign of the dipole moment changes.

**Anion States of the Film.** Figure 5 presents the TPPE signal observed for the various monolayers. In these experiments, the first photon injects an electron into the layer from the substrate, and the second photon ejects the electron from a metastable state on the layer to the vacuum. In the transfer from the gold substrate to the film, the electron loses energy by polarization relaxation in the layer. The measured kinetic energy,  $E_k$ , is given by  $E_k = h\nu - E_b$ , in which  $h\nu$  is the single photon energy and  $E_b$  is the binding energy (BE) of the metastable state relative to the vacuum level. This metastable state is the negative ion state on the layer, and it is common to assume that it correlates with the energy of the lowest unoccupied molecular orbital (LUMO).<sup>42</sup> The relaxation processes that occur in the layer distinguish this type of two-photon process from the coherent two-photon excitation of electrons from the metal's valence band to the vacuum. In the coherent process, the electron energy is equal to twice the photon energy less the WF.

In Figure 5, the signal observed with molecule **12** is the largest and its peak is the lowest in energy. The large amplitude implies a long lifetime for the trapped electron. In part, this long lifetime may result from the chain length of **12**. The large energy shift means that the electron injected into this layer is in the most stable state among the self-assembled monolayers (SAMs) studied. Molecules **5**, **7**, and **11** form a group that supports negative ion states, thus having signals larger than those of the other molecules, except **12**. The signals from molecules **3**, **6**, and **9** are significantly smaller than that of **12**, indicating that either the yield of trapped electrons or their lifetime in the layer is smaller. Also, the peaks of **3**, **6**, and **9** occur at higher energies, indicating that the negative ion state is less stable for these molecules. The low signal obtained for molecule **2** also indicates an unstable negative ion. Finally, molecules **4** and **10**

**TABLE 3: XPS Data for Three Representative Samples<sup>a</sup>**

molecule	$\Delta\text{WF}$ (meV)	$\text{C}^{\text{COO}}(1s)$ (eV)	$\Delta\Phi^{\text{COO}}$ (meV)	$\text{N}(1s)$ (eV)	$\Delta\Phi^{\text{end}}$ (meV)
#2	+30	288.95	−300	399.2	+120
#9	+600	288.6	+50	399.0	+570
#4	−320	288.55	+100		

<sup>a</sup> The average change in the WF difference values (given in meV) refers to a clean gold surface. The reference BE values,<sup>43</sup> used for derivation of local potential,  $\Delta\Phi$ , are 399.32 eV for sample #2, having nitrogen within the ring (sample #2); 399.57 eV for the triple bond nitrogen (sample #9); and 288.65 eV for a carboxylic carbon next to an aromatic ring (sample #4).

are borderline cases, with less stable negative ion states than those of the former molecules but more stable states than those of the molecules **2**, **3**, **6**, and **9**.

The TPPE data provide a hierarchy in terms of the stability of the negative ion state on the adsorbed layer, with molecule **12** being the most stable and molecule **9** the least stable.

**XPS Shifts.** The XPS spectra of the SAMs, in particular BEs of core electrons in specific atoms, contain detailed information about changes in the local electrostatic potential across an adsorbed molecule. Often, this information is obscured by chemical shifts and beam-induced charging effects. This local electrostatic information can be extracted from the XPS spectra if a reliable reference energy can be found. In the present work, in situ WF measurements are compared with the traditional XPS information to provide a self-consistent analysis of relative atomic line-shifts within the molecular monolayers. A detailed description of the method and the elimination of artifacts is given elsewhere.<sup>28</sup>

In the following, we analyzed in detail three samples, **2**, **4**, and **9**, which differ in their end-groups. Compounds **2** and **9** show reasonable agreement between the measured dipole in the layer and that calculated by the STO-3G/Mulliken method for the isolated molecule, whereas **4** displays a significant deviation for both calculation methods. By comparing the energy shifts of atomic spectral lines in similar bonding environments, we can assess the charge redistribution that occurs in the molecule. Table 3 presents the (in situ) XPS-derived WF values and the BEs of different core electrons in the molecules. The X-ray flux was kept low enough so that beam-induced charging could be neglected, as verified by complementary measurements. The presence of some OH contamination in part of the samples makes the O(1s) line hardly usable in the present analysis. It should be stressed that the BE reference values<sup>43</sup> used in Table 3 have been derived from bulk polymeric systems (using a different experimental configuration). The present samples, although their absolute BEs can be questioned, provide an internally consistent set for relative comparisons, which is preferred for fine analysis. The discussion below relies, therefore, on differences between the samples with minor usage of reference to the values from the literature. The sign for  $\Delta\text{WF}$  is chosen in such a way that the negative extra charge is assigned to a higher potential (and, hence, to higher WF), while it is associated with a lower BE.

Figure 6a compares XPS features of monolayer films **2** and **9**. An agreement is found (see also Table 3) between the difference in WF values of the two samples **2** and **9** and the difference in N(1s) BEs, namely, the BE shifts in the molecular end-groups, provided that the BE shifts are evaluated with respect to the actual chemical state of the nitrogen in each molecule. The local electrostatic potential ( $\Delta\Phi$ ) derived for the nitrogen site, Table 3, is given by the difference between the measured and reference values, 399.32–399.2 eV for molecule

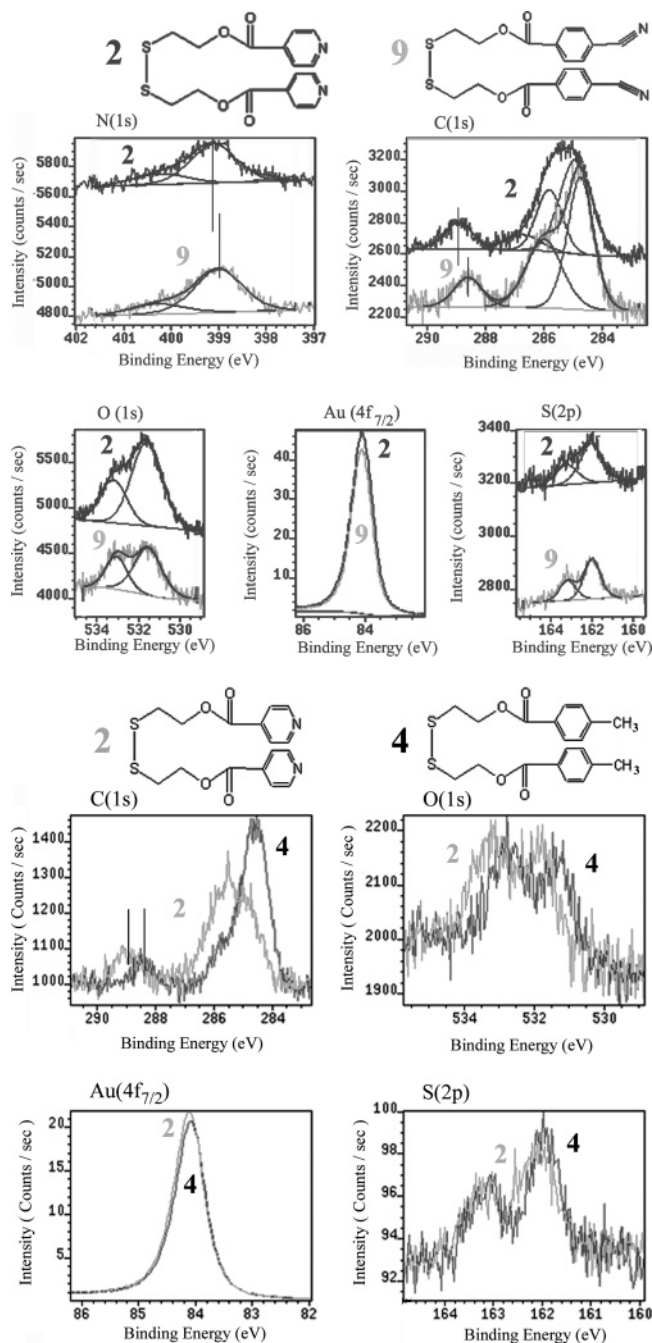


**Figure 6.** (a) XPS data comparing samples **2** and **9**. The core level spectra are shown. Note the similar peak positions for the gold and sulfur core lines, while the nitrogen and carbon BEs are different. (b) XPS data comparing samples **2** and **4**. The relative shift in the C(1s) feature around 289 eV is not a chemical shift. It reflects differences in the local potential. In contrast to Figure 3, the sign of this shift is opposite to that derived for the WF. The markers (vertical lines) in the spectrum refer to the N and C features discussed in the text.

**9** and 399.57–399.0 eV for **2**. Derivation of the local potential at the carboxylate carbon is simpler, as both molecules have chemically “identical” carboxylic carbons. We can, therefore, use this latter local electrostatic potential as an internally consistent reference for both **2** and **9**. The resultant difference in  $\Delta\Phi$  values at the carboxylic carbon, comparing molecules **2** and **9** (see also Figure 6a), is smaller than the difference at the nitrogen site (350 meV vs 450 meV). This fact suggests that molecule **9** has an integrally more negative charge and, more importantly, that this additional charge is located on the nitrogen.

This electrostatic difference is consistent with the negative ion state of the film composed of **9** being less stable than that formed from **2**.

The effect of molecular order on the surface dipoles has been further studied by shortening the adsorption time of molecule **9**. Instead of overnight adsorption periods, samples were prepared by dipping in solution for 10, 2.5, and 0.5 min. The results with the 10-min sample were similar to those of the standard preparation. With the 2.5-min sample, a small reduction in WF could already be observed. Upon 30-s adsorption, a dramatic change was found; the WF became equal to that of the reference gold, and the N(1s) and C(1s) BEs shifted correspondingly toward their “noncharged” values (ca. 450-meV shift of the nitrogen, as compared to that of the standard molecule **9** samples). The quantitative XPS analysis of this latter sample showed a smaller amount of adsorbed molecules (~30% less than the standard ones), some additional amount of extra oxygen, and a relatively small amount of extra carbon. This sample was also less stable under the X-ray beam. It is, therefore, suggested that the 0.5-min process is sufficient to efficiently cover the surface with the proper molecules; however, it is not long enough to achieve compact packing and orientational order.

Strikingly, in the case of a monolayer made from molecule **4**, a qualitatively different result is observed. Although the WF measured for the gold coated with molecule **4** is lower than that with **2**, its oxidized carbon signal (see Figure 6b) indicates a higher local potential (namely, lower BE) at the carboxylic group. This means that there is excess negative charge on the carboxylic group, while the end-group of **4** has a partial positive charge, as indicated by the change in the WF.

## Discussion

In trying to analyze the change occurring in the charge distribution of the adsorbed molecules, we compare our results to calculations of the dipole moment for the isolated molecules. Using different calculation methods and calibrating them against known values allows us to state that the dipole moment of the adsorbed molecules is reduced significantly relative to the magnitude of the dipole moment of the free molecule, for most cases. When the original dipole moment of the adsorbate points away from the surface (positive pole farther away than the negative pole), electrons are transferred from the substrate to the positive pole. When the dipole is pointing toward the substrate, the picture is usually more complex and involves charge reorganization in the molecule. In what follows, the mechanism responsible for these effects will be proposed and justified.

The change in the WF, and, hence, in the effective dipole moment of the adsorbed molecules, may be described by considering the effective dipole moment,  $\mu$ , to have two components: the component of the intrinsic dipole moment perpendicular to the surface,  $M_p$ , and a surface dipole moment,  $M_s$ , which results from charge redistribution (arising from polarization, from charge transfer between the substrate and the molecule, and/or from modification of the metal’s electron density tail at the surface).<sup>44</sup> Hence, the measured dipole moment may be written as

$$\mu = M_p + M_s \quad (2)$$

$M_s$  is the difference between  $\mu$  for molecules in the layer, extracted experimentally, and the value calculated for the free molecule,  $M_p$ .



A number of factors contribute to  $M_s$ . One contribution to  $M_s$  arises from the formation of the chemical bond between the adsorbate and the substrate. The sulfur binding group exhibits only small variations (compare the S(2p) core lines in Figure 6), far below the core level shifts of other atoms. Hence, the variation in WF for the different SAMs is not strongly linked to changes in the Au–S dipole. It necessarily arises from changes in the charge distribution further away from the gold substrate.

In the case of adsorbates with *electronegative* end-groups, the effect of electron transfer to the layer (see molecules **2**, **8**, and **9**) is small. For example, molecule **9**, as probed by the XPS spectra, appears to have most of its extra charge located at the end-groups. In addition, the measured WF is consistent with the one calculated by the STO-3G/Mulliken method and the electric field drops in this case almost linearly across the molecule. The exception is molecule **12**, which has a particularly large dipole, thus giving rise to a different effect, as explained below.

Our data show that molecules with *electropositive* end-groups exhibit electron transfer from the substrate to the molecule, so that  $M_s$  partially cancels  $M_p$ , making the effective dipole moment  $\mu$  smaller than  $M_p$ . Some direct evidence for attraction of substrate electrons toward the overlayer backbone is found in the XPS analysis of molecule **4**, where the carboxylic carbon exhibits an elevated potential, namely, the accumulation of *negative* charge. It seems that the charge transfer to molecule **6** is large enough to actually flip the sign of the dipole. The two-photon photoemission studies (Figure 4) show that the negative anion state is less stable for molecules **9**, **6**, **10**, and **4**, which means that these molecules are somewhat negatively charged.

Molecule **12** has a large intrinsic dipole moment of about 4.5 D with its negative pole away from the surface. Naively, such a molecule, when adsorbed almost perpendicular to the surface normal, should increase the WF. However, the adsorption of this molecule actually decreases the observed WF (see Table 1 and Figure 2). The effective dipole moment of this molecule (assuming a tilt angle of about 30°) changes from about 4.5 D to about –1.5 D. This change implies that negative charge is transferred from the imidazole to the gold substrate. This conclusion is consistent with the observations in Figure 5. Since electron donation to the substrate leaves the outer part of the layer with an excess positive charge, the electrons injected into the layer are stabilized. Figure 5 indicates that the BE of the extra electron to a layer made from molecule **12** is about 3.2 eV. In principle, this energy can be composed from two components, the molecular binding and the image charge effect due to the metal substrate. Since the substrate is identical for all SAMs and the image charge effect is weaker for the longer chain of **12**, the extra stability of the electron on molecule **12** must arise from the molecular effect. A similar phenomenon occurs for molecule **5**, but here, since the original dipole is much smaller, less charge is transferred to the substrate. It is important to realize that what seems to be a dramatic change in the dipole moment requires the transfer of only about 5% of an electron charge per molecule.

The question remains, What drives the significant charge redistribution in the molecules adsorbed as close-packed organized monolayers? The answer may lie in the dimensionality of the layer. When a macroscopic two-dimensional dipole layer is formed from strongly dipolar molecules, the electrostatic energy associated with it can be enormous. When such electrostatic forces become large enough, the charge redistributes

and reduces the electrostatic energy by requiring that the dipole–dipole interaction between the adsorbed molecules be minimized.<sup>21,22</sup> For highly polarizable adsorbate molecules, this process can occur by depolarization of the molecules. However, if the adsorbed molecules have low polarizability, the most energetically favorable mechanism for reducing the electrostatic energy is charge exchange with the substrate.<sup>22</sup> The charge exchange process is not necessarily symmetric for electrons transferred from the metal to the layer or vice versa. Since the WF of the substrate is about 5 eV, while the ionization energy of the molecules is of the order of 10 eV and more, one would expect that transferring electrons from the substrate to the layer would be easier than the reverse process, as is observed.

By comparing the WF differences between a large number of organic thiols, it is evident that the change in the total surface dipole moment is a complex phenomenon resulting from various coupled effects. The drive to reduce the dipole–dipole repulsion between the adsorbed molecules causes both charge redistribution in the molecules and charge transfer between the substrate and the adsorbed layer. The ability to compare similar molecules, all binding to the surface in the same way, shows that the organization itself involves charge transfer and formation of the surface potential. This effect is expected to occur only if the molecules are adsorbed as a close-packed layer, where the electrostatic repulsion between the parallel dipole moments can promote this “organization-induced charge transfer”.<sup>22</sup> In this respect, the disordered film experiment should provide additional evidence for the critical role of organization in dictating the surface dipole moment. The observation differs from that discussed in the past regarding atomic adsorbates because, in the molecular monolayers, the molecular intrinsic dipole moment may drive the charge redistribution and may play an important role in defining the dipole density.

**Acknowledgment.** We acknowledge partial support from the US–Israel Binational Science Foundation.

## References and Notes

- (1) (a) Gurney, R. W. *Phys. Rev.* **1935**, *47*, 479. (b) Ueba, H. *Surf. Sci.* **1991**, *242*, 266. (c) Albano, E. V. *Appl. Surf. Sci.* **1982**, *14*, 183. (d) Lang, N.; Kohn, W. *Phys. Rev. B* **1970**, *1*, 4555.
- (2) Kruger, J.; Bach, U.; Graetzel, M. *Adv. Mater.* **2000**, *12*, 447.
- (3) (a) Katz, H. E.; Johnson, J.; Lovinger, A. J.; Li, W. *J. Am. Chem. Soc.* **2000**, *122*, 7787. (b) Appleyard, S. F. J.; Day, S. R.; Pickford, R. D.; Willis, M. R. *J. Mater. Chem.* **1999**, *10*, 169. (c) Campbell, I. H.; Rubin, S.; Zawodzinski, T. A.; Kress, J. D.; Martin, R. L.; Smith, D. L. *Phys. Rev. B* **1996**, *54*, 14321.
- (4) (a) Dmitriev, S. G.; Kogan, S. M. *Sov. Phys., Solid State* **1979**, *21*, 17. (b) Kim, C. W.; Villagran, J. C.; Even, U.; Thompson, J. J. *Chem. Phys.* **1991**, *94*, 3974.
- (5) Briggs, D.; Seah, M. P. *Practical Surface Analysis*, 2nd ed.; Wiley: New York, 1994; Vol. 1.
- (6) (a) Ishii, H.; Sugiyama, K.; Ito, E.; Seki, K. *Adv. Mater.* **1999**, *11*, 605. (b) Broughton, J. Q.; Perry, D. L. *Surf. Sci.* **1978**, *74*, 307. (c) Brundle, C. R. *Surf. Sci.* **1975**, *48*, 99. (d) Gadzuk, J. W. *Phys. Rev. B* **1976**, *14*, 2267.
- (7) Mönch, W. *Semiconductor Surfaces and Interfaces*, 3rd ed.; Springer: New York, 2001; Chapter 14.
- (8) Ishii, H.; Sugiyama, K.; Ito, E.; Seki, K. *Adv. Mater.* **1999**, *11*, 605.
- (9) Yaliraki, S. N.; Roitberg, A. E.; Gonzalez, C.; Mujica, V.; Ratner, M. A. *J. Chem. Phys.* **1999**, *111*, 6997.
- (10) Vilan, A.; Shanzer, A.; Cahen, D. *Nature* **2000**, *404*, 166.
- (11) Campbell, I. H.; Kress, J. D.; Martin, R. L.; Smith, D. L.; Barashkov, N. N.; Ferraris, J. P. *Appl. Phys. Lett.* **1997**, *71*, 3528.
- (12) Hill, I. G.; Milliron, D.; Schwartz, J.; Kahn, A. *Appl. Surf. Sci.* **2000**, *166*, 354.
- (13) Collier, C. P.; Wong, E. W.; Belohradsky, M.; Raymo, F. M.; Stoddart, J. F.; Kuekes, P. J.; Williams, R. S.; Heath, J. R. *Science* **1999**, *285*, 391.
- (14) Chen, J.; Reed, M. A.; Rawlett, A. M.; Tour, J. M. *Science* **1999**, *286*, 1550.

- (15) Vuillaume, D.; Chen, B.; Metzger, R. M. *Langmuir* **1999**, *15*, 4011.
- (16) Punkka, E.; Rubner, R. F. *J. Electron. Mater.* **1992**, *21*, 1057.
- (17) See for example: Yamamori, A.; Hayashi, S.; Koyama, T.; Taniguchi, Y. *Appl. Phys. Lett.* **2001**, *78*, 3343–3345. Crone, B. K.; Davids, P. S.; Campbell, I. H.; Smith, D. L. *J. Appl. Phys.* **2000**, *87*, 1974.
- (18) Wu, D. G.; Cahen, D.; Graf, P.; Naaman, R.; Nitzan, A.; Shvarts, D. *Chem.—Eur. J.* **2001**, *7*, 1743.
- (19) Nitzan, A.; Benjamin, I. *Acc. Chem. Res.* **1999**, *32*, 854.
- (20) Hutchison, G. R.; Ratner, M. A.; Marks, T. J.; Naaman, R. *J. Phys. Chem. B* **2001**, *105*, 2881.
- (21) Vager, Z.; Naaman, R. *Chem. Phys.* **2002**, *281*, 305.
- (22) Lvov, V. S.; Naaman, R.; Tiberkevich, V.; Vager, Z. *Chem. Phys. Lett.* **2003**, *381*, 650.
- (23) Boker, R. D.; McConnell, H. M. *J. Phys. Chem.* **1993**, *97*, 13419.
- (24) Möhwalld, H. *Annu. Rev. Phys. Chem.* **1990**, *41*, 441.
- (25) Alloway, D. M.; Hofmann, M.; Smith, D. L.; Gruhn, N. E.; Graham, A. L.; Colorado, R., Jr.; Wysocki, V. H.; Lee, T. R.; Lee, P. A.; Armstrong, N. R. *J. Phys. Chem. B* **2003**, *107*, 11690.
- (26) (a) Naaman, R.; Vager, Z. *Acc. Chem. Res.* **2003**, *36*, 291. (b) Naaman, R.; Haran, A.; Nitzan, A.; Evans, D.; Galperin, M. *J. Phys. Chem. B* **1998**, *102*, 3658.
- (27) Kronik, L.; Shapira, Y. *Surf. Sci. Rep.* **1999**, *37*, 1.
- (28) Cohen, H.; Noguez, C.; Zon, I.; Lubomirsky, I. *J. Appl. Phys.* **2005**, *97*, 113701.
- (29) Liu, H.; Yamamoto, H.; Wei, J.; Waldeck, D. H. *Langmuir* **2003**, *19* (6), 2378.
- (30) Bibart, R. T.; Vogel, K. W.; Drueckhammer, D. G. *J. Org. Chem.* **1999**, *64*, 2903.
- (31) Yamamoto, H.; Liu, H.; Waldeck, D. H. *J. Chem. Soc., Chem. Commun.* **2001**, 1032.
- (32) Wei, J.; Liu, H.; Dick, A. R.; Yamamoto, H.; He, Y.; Waldeck, D. H. *J. Am. Chem. Soc.* **2002**, *124*, 9591.
- (33) Ron, H.; Matlis, S.; Rubinstein, I. *Langmuir* **1998**, *14*, 1116–1121.
- (34) For samples **1** and **5**, some extra carbon was detected. We attributed this result to incomplete adsorption of the studied molecules, with other hydrocarbons adsorbed at the “open” areas. Alternatively, the extra carbon may be associated with hydrocarbons adsorbed on top of the studied layer. Obviously, with diluted dipolar molecules, the measured WF should be affected; most likely, it is reduced in magnitude. Experimentally, we could not differentiate this effect from the main one of charge transfer, which acts in the same direction. A rough estimate would suggest that the dipole magnitude of perfect monolayers might increase in the case of molecules **1** and **5** by a factor of two, at most. Note that such corrections do not contradict any of the conclusions.
- (35) To achieve a high level of quantification, we used repetitive XPS scans over many hours (up to 24 h in some cases), while the WF measurements were always less than 1 h, usually the early 10–20 min of each experiment. On a time scale of ~5 h of irradiation, relative changes in atomic concentrations,  $\Delta I/I$ , were in most samples less than 5%. In samples **5** and **12**, we observed a bit higher degradation rates, about 8–10% during 5–6 h of irradiation. It is stressed that the WF measurements were also repeated. We could, therefore, directly quantify the influence of degradation on the measured WF and, hence, eliminate these effects by extrapolating to time zero when necessary.
- (36) Schmidt, M. W.; Baldrige, K. K.; Boatz, J. A.; Elbert, S. T.; Gordon, M. S.; Jensen, J. H.; Koseki, S.; Matsunaga, N.; Nguyen, K. A.; Su, S. J.; Windus, T. L.; Dupuis, M.; Montgomery, J. A. *J. Comput. Chem.* **1993**, *14*, 1347–1363.
- (37) Pu, J.; Thomson, J. D.; Xidos, J. D.; Li, J.; Zhu, T.; Hawkins, G. D.; Chuang, Y.-Y.; Fast, P. L.; Liotard, D. A.; Rinaldi, D.; Gao, J.; Cramer, C. J.; Truhlar, D. G. *GAMESSPLUS*, version 4.3.1; University Of Minnesota: Minneapolis, MN, 2004; based on GAMESS as described in ref 36.
- (38) Zhu, J. L. T.; Cramer, C. J.; Truhlar, D. G. *J. Phys. Chem. A* **1998**, *102*, 1820.
- (39) For references describing the standard abbreviations and basic ab initio methods, see the following: (a) Hehre, W. J.; Radom, L.; Schleyer, P. v. R.; Pople, J. A. *Ab initio Molecular Orbital Theory*; Wiley-Interscience: New York, 1986. (b) Clark, T. *A Handbook of Computational Chemistry*; Wiley-Interscience: New York, 1985.
- (40) Wu, D.; Ghabboun, J.; Martin, J.; Cahen, D. *J. Phys. Chem. B* **2001**, *105*, 12011.
- (41) This value is based on the spectroscopic ellipsometry measurement where the ellipsometric parameters for the monolayers ( $\Delta$  and  $\Psi$ ) were fitted by a Cauchy model over a wide range of wavelengths (400–900 nm) and the refractive index ( $n + ik$ ) of the monolayers was obtained. For  $\lambda = 638.2$  nm the value of the refractive index for all the molecules was found to be  $n \approx 1.48$  and  $k = 0$ . Hence, the dielectric constant is  $\epsilon \approx n^2 \approx 2.2$ .
- (42) The electron is bound by both the image potential from the metal and the molecular potential. For similarly sized molecules and film dielectric properties, the image potential with the gold should be similar and the BE shifts would correlate with the electron affinity of the molecules, i.e., the LUMO in the limit of Koopmans theorem. For details, please see: (a) Wang, H.; Dutton, G.; Zhu, X.-Y. *J. Phys. Chem. B* **2000**, *104*, 10332–10338. (b) Zhu, X.-Y. *Annu. Rev. Phys. Chem.* **2002**, *53*, 221–247.
- (43) Beamson, G.; Briggs, D. *High-Resolution XPS of Organic Polymers. The Scienta ESCA300 Database*; Wiley & Sons: Chichester, U.K., 1992.
- (44) Crispin, X.; Geskin, V.; Crispin, A.; Cornil, J.; Lazzaroni, R.; Salaneck, W. R.; Brédas, J.-L. *J. Am. Chem. Soc.* **2002**, *124*, 8131.